

Optically induced splitting of bright excitonic states in coupled quantum microcavities

A. Armitage and M. S. Skolnick

Department of Physics, University of Sheffield, Sheffield S3 7RH, United Kingdom

V. N. Astratov

*Department of Physics, University of Sheffield, Sheffield S3 7RH, United Kingdom
and A. F. Ioffe Physico-Technical Institute, 194021 St. Petersburg, Russia*

D. M. Whittaker

Toshiba Cambridge Research Centre, Cambridge CB3 0HE, United Kingdom

G. Panzarini and L. C. Andreani

INFN, Dipartimento di Fisica "A. Volta," Università di Pavia, 27100 Pavia, Italy

T. A. Fisher

Department of Electrical and Electronic Engineering, University of Western Australia, Nedlands WA6907, Australia

J. S. Roberts

Department of Electronic and Electrical Engineering, University of Sheffield, Sheffield S1 3JD, United Kingdom

A. V. Kavokin

Dipartimento di Ingegneria Elettronica, Università di Roma II, 00133 Roma, Italy

M. A. Kaliteevski

A. F. Ioffe Physico-Technical Institute, 194021 St. Petersburg, Russia

M. R. Vladimirova

Dipartimento di Ingegneria Elettronica, Università di Roma II, 00133 Roma, Italy

(Received 27 February 1998)

Optically induced lifting of the degeneracy of spatially separated quantum-well excitons is reported from angular-dependent studies of coupled-quantum-microcavity structures. Interaction between the symmetric and antisymmetric photon modes of the coupled cavity and the corresponding combinations of the degenerate excitonic states gives rise to two bright excitons with a sizeable splitting of several meV, which together with the cavity modes lead to four dips in reflectivity spectra. In the near-resonance regime, evidence for motional narrowing of the polariton spectra is found.

[S0163-1829(98)06320-6]

The simultaneous confinement of electronic states and optical fields in quantum microcavity structures (QMCs) has opened up a very promising field of research allowing new means to control the light-matter interaction in solids.^{1,2} The quantized photon modes of the microcavity and the exciton states of quantum wells (QW's) embedded in the QMC represent an interesting physical example of a system of coupled oscillators. Strong coupling between the two oscillators arises in the resonance regime, leading to the formation of new exciton-photon coupled modes, termed cavity polaritons.

When two (or several) identical QW's are placed in a QMC the vacuum Rabi splitting (Δ_{VRS}) is increased but only a single material excitation can be seen. In general, the excitonic states of two identical QW's not embedded in a QMC can be classified in terms of symmetric (*S*) and antisymmetric (*AS*) states, which have a radiative splitting due to interwell dipolar coupling;³ the splitting is of the order of a frac-

tion of an meV and is therefore easily washed out by disorder. When the two identical QW's are embedded in a single QMC in the strong-coupling regime only one of the *S* and *AS* excitonic states is maximally coupled to light and observable.⁴ Similarly, the radiative splitting in multiple QW's (Ref. 5) is usually suppressed by disorder; *N* identical excitons in a QMC give rise to a single "bright" state, and *N* - 1 unobservable "dark" states.⁶ Thus only one excitation can be detected at a time even when two or more oscillators are present; neither a radiative splitting between bright excitonic states, nor any effect related to dark states has been observed up to now.

In the present work we show that specially designed systems containing more than one cavity with embedded QW's allow a *sizeable* (several meV) radiative splitting to be achieved between *bright* excitonic states. Optically induced coupling, and hence splitting, between excitons confined in separate cavities is achieved over very large, macroscopic

distances ($>2 \mu\text{m}$) as a result of the symmetry properties of the long-wavelength, long-coherence-length optical fields. The removal of degeneracy has analogous features in purely electronic systems like double QW's and superlattices,⁷ where, however, the interaction length is typically less than 5 nm as determined by quantum-mechanical tunneling of the electronic wave functions.

It has been demonstrated previously that coupled QMC's lead to an optical splitting (Δ_{SAS}) between S and AS cavity modes,⁸ and even to dual lasing⁹ due to long-range optical coupling. Cavity-induced interaction between localized oscillators has also been studied in the context of models for lateral disorder.¹⁰ In these studies the excitonic state appeared as a single, unsplit oscillator. In fact when $\Delta_{\text{SAS}} \gg \Delta_{\text{VRS}}$, as in Ref. 8, the S and AS exciton states come into resonance with each coupled cavity mode separately and the lifting of the exciton degeneracy does not occur. It does not arise either when $\Delta_{\text{VRS}} \gg \Delta_{\text{SAS}}$, since then there is negligible coupling between the cavities. The present structure is specifically designed to achieve splitting between the coupled optical modes of the same order as Δ_{VRS} . A large splitting of spatially separated bright exciton states is then achieved via their interaction with confined optical eigenmodes of the same symmetry. Under resonance conditions, the coupling of S and AS cavity modes with the excitons yields four polariton states that are detected as distinct features in reflectivity spectra. In the time domain, the coherent phenomena correspond to the photon-mediated oscillation of excitation between macroscopically separated exciton states. As a result of the symmetry properties of its optical modes the coupled QMC thus leads to qualitatively new physics compared to, for example, the single QMC containing two QW's,⁴ where if the QW excitons have the same energy one of the two excitonic states remains dark and unobservable.

QMC's are planar Fabry-Pérot cavities whose optical lengths are equal to an integral number of half wavelengths ($n\lambda/2$) of the exciton transitions of QW's embedded in the cavity. The high reflectivity mirrors are formed by distributed Bragg reflectors (DBR's), alternate $\lambda/4$ layers of high and low refractive index. A schematic diagram of the two period coupled QMC employed here is shown in Fig. 1(a). It consists of two GaAs cavities, each one λ thick, and three sets of GaAs/AlAs DBR's. In a single cavity, the optical field strength in the cavity is enhanced relative to that of the external photon field. In a coupled cavity the same phenomenon arises, but in addition there is coupling between the photon fields of the two cavities, as shown in Fig. 1(b); S and AS photon fields result with the coupling strength controlled by the transmission of the central mirror. The QMC investigated was grown by metal-organic vapor phase epitaxy (MOVPE). The lowest GaAs/AlAs DBR contains 17.5 layer repeats, the center 14.5 and the top 12 repeats. Each GaAs cavity contains three 100-Å $\text{In}_{0.06}\text{Ga}_{0.94}\text{As}$ QW's, 100 Å apart, resulting in negligible electronic coupling. The nominal 1λ cavity lengths were 2500 Å. A piece of the wafer with average cavity energies at normal incidence ~ 15 meV below that of the QW excitons was employed.

To tune the interaction and to achieve resonance between the coupled cavity modes and the QW exciton angle-dependent reflectivity techniques were employed. The cavity mode energy of a QMC depends strongly on the external

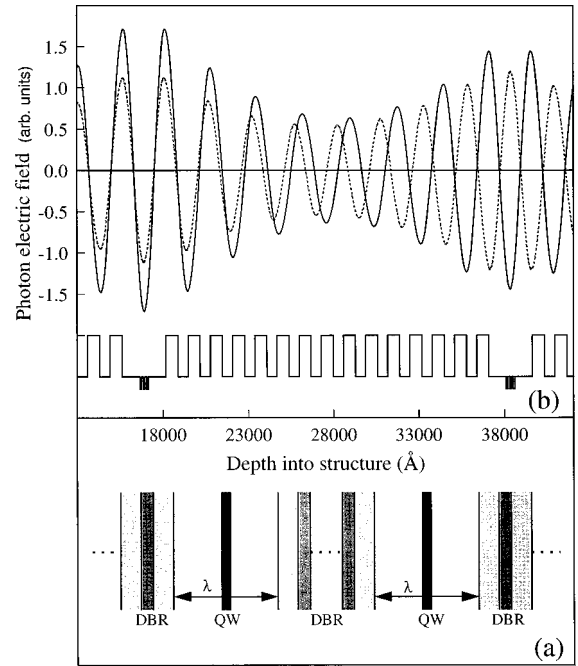


FIG. 1. (a) Schematic diagram of coupled quantum microcavity. (b) Symmetric (full) and antisymmetric (dashed) photon fields, calculated using transfer matrix reflectivity techniques for cavities of slightly different lengths, as in the present structure.

angle of incidence (θ),¹¹ the energy at angle θ being given by $E(\theta) = E_0[1 - (\sin^2\theta/n^2)]^{-1/2}$, where E_0 is the energy at $\theta = 0$ and n is an average refractive index. Variation of θ from 0 to 50° leads to an increase of $E(\theta)$ by ~ 35 meV, and permits tuning of the cavity modes through the angle-independent exciton features. White light illumination from a tungsten-halogen lamp was employed. The reflected light was dispersed by a 0.75-m spectrometer and detected by a Ge photodiode.

A series of unpolarized reflectivity spectra taken at 10 K is shown in Fig 2 for angles of incidence from 10 to 51.5° . At low θ the two coupled cavity dips are observed, labeled C_S and C_{AS} , respectively, together with a weak exciton feature (X) to higher energy. With increasing θ the C_S , C_{AS} dips shift to higher energy and move into the interacting resonance regime with the exciton feature. From 20 to 33° the exciton peak splits into two bright states and a four-dip spectrum is observed; the lifting of the degeneracy of spatially separated exciton states has been achieved, and the splitting of the bright excitons is in the meV range. For $\theta > 35^\circ$ the cavity modes have moved to higher energy than the exciton, and the three-dip spectrum is restored, with the exciton feature weakening as it moves out of resonance. The dip energies are plotted versus θ in Fig. 3, the transition from three dips at low θ , to four dips on resonance, back to three dips at high θ being clearly visible. Anticrossing between the coupled cavities and the exciton features is observed in the 25– 40° range, the characteristic behavior of coupled modes in a strongly interacting regime.

The physical behavior in the resonance regime can be understood by considering the cavity and exciton modes as a four oscillator system; this description can be derived rigorously from an analytic treatment of semiclassical light-matter

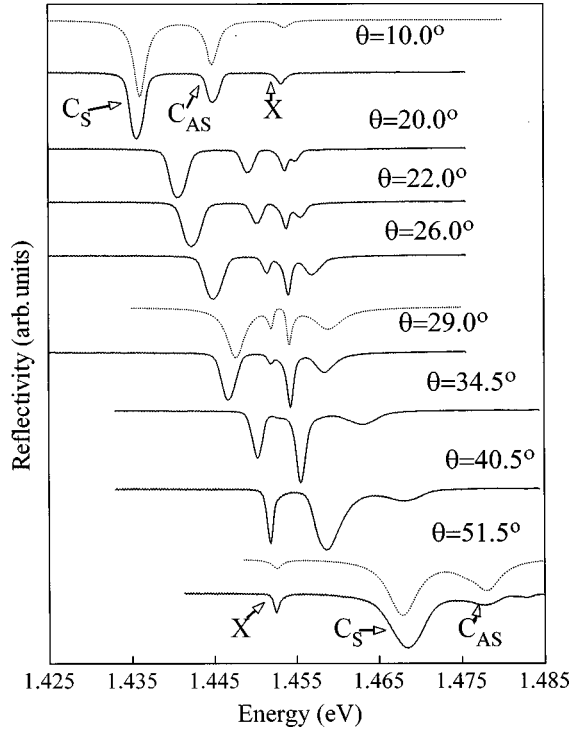


FIG. 2. Reflectivity spectra (full lines) as a function of angle of incidence θ . At low angles the symmetric and antisymmetric photon modes, labeled C_S and C_{AS} , are observed, with the exciton dip (X) to higher energy. In the strongly interacting regime from 20° to 29° four features are seen, due to lifting of the degeneracy of the exciton states. For $\theta > 35^\circ$, three peaks are again observed. All spectra are on the same vertical scale, the C_S dip at $\theta = 10^\circ$ corresponding to a 40% decrease in reflectivity from the near 100% value in the high reflectivity region. The dotted lines are TMR fits to the 10° , 29° , and 51.5° spectra. The 10° and 51.5° fits employ an exciton linewidth of 0.9 meV, whereas for 29° a width of 0.3 meV is used. The weak feature at 1.482 eV in the 51.5° spectrum probably arises from interaction with quantum-well excited states.

interaction.¹² The optical fields in the cavities, considered for the moment to have equal lengths, couple to give the S and AS cavity modes. The coupled cavity energies are obtained from diagonalization of the Hamiltonian,

$$\begin{pmatrix} E_c & V_{\text{opt}} \\ V_{\text{opt}} & E_c \end{pmatrix}, \quad (1)$$

where E_c is the energy of the uncoupled modes and $V_{\text{opt}} = \hbar c \sqrt{1 - R_c} / (2nL_{\text{eff}} \cos \theta_c)$ is the optical coupling between the cavities, determined by the transmission $1 - R_c$ of the central mirror ($L_{\text{eff}} \approx 1 \mu\text{m}$ is the effective cavity length including DBR phase delay, and θ_c is the internal angle). The energies of the coupled cavity modes are given by $E_{S,AS} = E_c \pm V_{\text{opt}}$, with splitting $\Delta_{SAS} = 2V_{\text{opt}}$.

The exciton states in the two separate cavities also form symmetric and antisymmetric combinations (ψ_S, ψ_{AS}), which are degenerate to a very good approximation. The S coupled cavity mode couples only to the S exciton state ψ_S and likewise C_{AS} couples only to ψ_{AS} . The energies (E) of the coupled polariton states, neglecting damping, are given by the solutions of

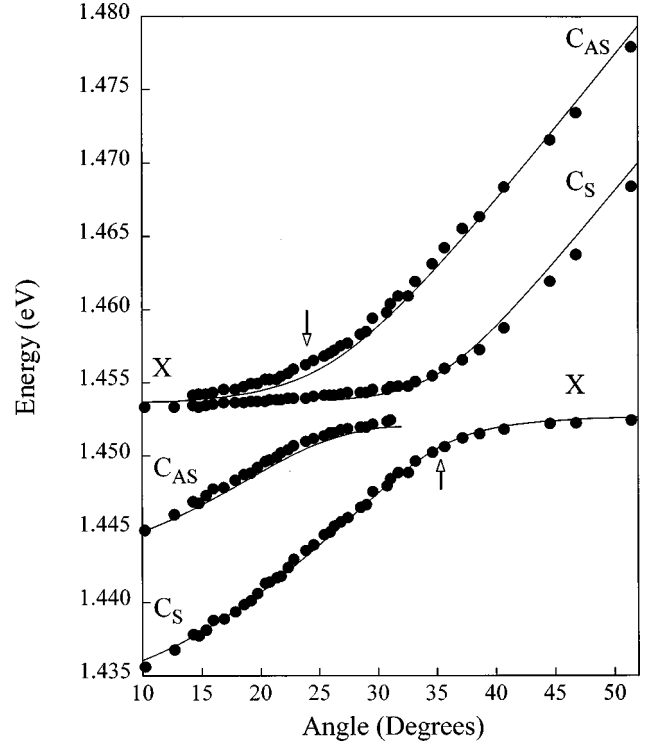


FIG. 3. Dip positions of Fig. 2 plotted as a function of angle of incidence. The lines are calculated from the transfer matrix model. Anticrossings between the antisymmetric exciton/cavity modes at 24° and between the symmetric combination at 35° are indicated by arrows.

$$(E_S - E)(E_x - E) = V_{xc}^2, \quad (2)$$

$$(E_{AS} - E)(E_x - E) = V_{xc}^2, \quad (3)$$

obtained from diagonalization of 2×2 Hamiltonians very similar to Eq. (1), but with the E_c on the first row replaced by E_S or E_{AS} , and E_c on the second row replaced by E_x , the unperturbed exciton energy. $V_{xc} = [2\pi e^2 \hbar^2 N_{\text{eff}} f_{xy} / (n^2 m L_{\text{eff}})]^{1/2}$ is the exciton-photon coupling potential ($2V_{xc} = \Delta_{\text{VRS}}$) expressed in terms of the oscillator strength per unit area f_{xy} and an effective number N_{eff} of QW's.¹³ The solutions of Eqs. (2) and (3) give rise to four distinct eigenvalues; the degeneracy of the exciton states derived from the QW's in the two cavities is lifted by coupling to the S and AS photon modes of the coupled cavities.

The four oscillator model permits a good physical understanding of the on-resonance behavior. In particular, it accounts for the presence of four reflectivity peaks in the resonance regime. Due to the splitting between S and AS cavity modes, anticrossing between the AS exciton and cavity states occurs at an angle $\theta \approx 24^\circ$, while the anticrossing between the S exciton and cavity states takes place at $\theta \approx 35^\circ$. Using an exciton oscillator strength $f_{xy} = 4.2 \times 10^{12} \text{ cm}^{-2}$ for the 100-Å-wide $\text{In}_{0.06}\text{Ga}_{0.94}\text{As}$ QW's,¹⁴ and $N_{\text{eff}} = 2.52$ for each set of three QW's, the Rabi splitting is calculated to be $\Delta_{\text{VRS}} = 2V_{xc} = 4.9 \text{ meV}$, in good agreement with experiment.¹⁵ Also, the reflectivity of the central mirror is $R_c = 0.97$, leading to an optical splitting $\Delta_{SAS} \approx 10 \text{ meV}$: this agrees well with the experimental splitting between AS and S cavity modes at low ($\theta = 10^\circ$) or high ($\theta = 51.5^\circ$) angle. It

is important to note that off-resonance (at, e.g., 10° and 51.5°) only one exciton feature is observed, with linewidth 0.9 meV [full width at half maximum (FWHM)]. This shows that the excitonic energies in the QW's are equal to within ~ 0.5 meV, and that the splitting on resonance arises from optically induced coupling, and not from energy differences between the wells, or from direct electronic coupling between them.¹⁶

To obtain a quantitative understanding of the spectra, transfer matrix reflectivity (TMR) simulations¹⁷ were carried out, with the excitons treated as Lorentz oscillators. TMR fits to the 10° , 29° , and 51.5° spectra are shown by the dashed lines on Fig. 2, and the dip energies as a function of θ by the full lines on Fig. 3. The TMR simulations permit the optical fields to be calculated; the photon fields in Fig. 1(b) were calculated at the energies of the 10° C_S and C_{AS} dips (Fig. 2), with C_S calculated to lie at lower energy than C_{AS} . To fit the relative intensities of the cavity peaks at 10° it was necessary to unbalance the cavities very slightly, with the upper cavity 0.6% longer than the lower cavity.¹⁸ For equal cavity lengths the two dips are found to have very nearly equal intensities, even in the presence of cavity absorption. Uniform cavity absorption, leading to reduced finesse, was included to fit the cavity linewidths (FWHM) of ~ 1.8 meV. With these small adjustments, and the exciton energy and width chosen to agree with experiment, the good fit to the 10° spectrum (Fig. 2) was obtained.¹⁹

The same set of parameters explain well the variation of the dip positions with angle (the full lines in Fig. 3). In particular, the on-resonance anticrossing and the lifting of the degeneracy of the exciton states is reproduced very well. The values employed for the interaction potentials are $V_{\text{opt}}=4.6$ meV and $V_{\text{xc}}=2.5$ meV, respectively, close to those calculated above. As discussed in Ref. 12, the energy dependence of the refractive index¹⁹ is essential in order to obtain the correct polariton dispersion at large angles. At high angle ($>40^\circ$), the cavity peaks show significant broad-

ening, with linewidths a factor of 2.5 greater than those at low θ . The increased widths arise since for $\theta > 40^\circ$, the $C_S C_{AS}$ modes fall into the energy range of the excitonic continuum.^{20,21} A good fit to the 51.5° spectrum (see Fig. 2) is obtained with inclusion of additional absorption in the QW regions of 0.6% per QW, a very reasonable value for the continuum absorption of a 100-Å QW.²²

We also obtain a very reasonable fit to the near-resonance spectrum at 29° (see Fig. 2), but only by using an exciton linewidth (ΔE_x) of 0.3 meV as opposed to the $\Delta E_x=0.9$ meV (Ref. 19) employed for the 10° and 51.5° fits. It is seen that the intensity distribution of the spectrum is reproduced well, with the third dip in order of increasing energy significantly deeper than the neighboring features. In addition, the simulated width of the third dip (0.9 meV) agrees with that observed (0.9 meV). If instead the $\Delta E_x=0.9$ meV of the off-resonance fits is employed, then the dip has width 1.5 meV, significantly greater than in experiment, and, furthermore, its depth is reduced relative to the other features. This need to employ narrow exciton linewidths in the resonance regime is consistent with recent observations of single QMC's, where motional narrowing (MN) of exciton disorder broadening, arising from the very strong polariton dispersion in the mixed mode regime, was shown to lead to narrow on-resonance linewidths.²³ The present results suggest that MN is also important in the present more complex four-mode system.

In conclusion, the optically induced splitting of bright exciton states separated by macroscopic distances of over $2 \mu\text{m}$ has been reported. The symmetry properties of the optical modes in the coupled QMC play a fundamental role in the achievement of a large radiative splitting. Control of the macroscopic coupling has been achieved by the use of angle tuning techniques. Good theoretical understanding of the reflectivity spectra and of the polariton energies has been obtained.

¹C. Weisbuch, M. Nishioka, A. Ishikawa, and Y. Arakawa, *Phys. Rev. Lett.* **69**, 3314 (1992).

²For a review of QMC physics see V. Savona, C. Piermarocchi, A. Quattropani, P. Schwendimann, and F. Tassone, in *New Aspects in Optical Properties of Materials*, Special Issue of Phase Transitions (Gordon and Breach, New York, 1997).

³D. S. Citrin, *Phys. Rev. B* **49**, 1943 (1994).

⁴G. Panzarini and L. C. Andreani, *Phys. Rev. B* **52**, 10 780 (1995); E. L. Ivchenko *et al.*, *J. Opt. Soc. Am. B* **13**, 1061 (1996); V. M. Agranovich, H. Benisty, and C. Weisbuch, *Solid State Commun.* **102**, 631 (1997). As these papers show, both material excitations become optically active if the two QW excitons have different energies.

⁵D. S. Citrin, *Solid State Commun.* **89**, 139 (1994); L. C. Andreani, *Phys. Status Solidi B* **188**, 29 (1995); G. Bjork *et al.*, *Phys. Rev. B* **52**, 17 310 (1995).

⁶G. C. La Rocca, F. Bassani, and V. M. Agranovich, *J. Opt. Soc. Am. B* **15**, 652 (1998).

⁷See, e.g., G. Bastard, in *Wave Mechanics Applied to Semiconductor Heterostructures*, Les Editions de Physique (Wiley, New York, 1988).

⁸R. P. Stanley, R. Houdré, U. Oesterle, M. Ilegems, and C. Weisbuch, *Appl. Phys. Lett.* **65**, 2093 (1994).

⁹P. Pellandini *et al.*, *Appl. Phys. Lett.* **71**, 864 (1997).

¹⁰R. Houdré, R. P. Stanley, and C. Weisbuch, *Phys. Rev. A* **53**, 2711 (1996); V. Savona and C. Weisbuch, *Phys. Rev. B* **54**, 10 835 (1996).

¹¹R. Houdré *et al.*, *Phys. Rev. Lett.* **73**, 2043 (1994).

¹²G. Panzarini and L. C. Andreani (unpublished).

¹³V. Savona *et al.*, *Solid State Commun.* **93**, 733 (1995).

¹⁴R. C. Iotti and L. C. Andreani, *Phys. Rev. B* **56**, 3922 (1997).

¹⁵A very similar value for V_{xc} is found for single QMC's of similar design, T. A. Fisher *et al.*, *Phys. Rev. B* **53**, R10 469 (1996).

¹⁶Electronic coupling between the wells in the same cavity will give rise to a splitting of 3 meV between the exciton states. However, only one of these states, the lowest-energy symmetric combination, has strong overlap with the photon field and is observable.

¹⁷M. Born and E. Wolf, *Principles of Optics* (Pergamon, New York, 1964).

¹⁸The 0.6% difference in the two cavity lengths is well within the expected accuracy of the MOVPE growth.

¹⁹The fit parameters were upper and lower cavity lengths 2536 and 2521 Å, DBR layer thicknesses 595 Å (GaAs), 703 Å (AlAs), background absorption coefficient 700 cm^{-1} , exciton energy in upper cavity $E_x = 1452.3 \text{ meV}$, E_x in lower cavity 1453.6 meV, and off-resonance exciton linewidth 0.9 meV. Wavelength-dependent refractive indices, taken from the 300-K data of J. T. Boyd, IEEE J. Quantum Electron. **8**, 788 (1972) were employed, reduced by 1.3% for use at 10 K.

²⁰J. Tignon *et al.*, Phys. Rev. Lett. **74**, 3967 (1995).

²¹The exciton binding energy is $\sim 8 \text{ meV}$, R. Atasonov *et al.*, Phys. Rev. B **50**, 14 381 (1994).

²²W. T. Masselink *et al.*, Phys. Rev. B **32**, 8027 (1985).

²³D. M. Whittaker, P. Kinsler, T. A. Fisher, M. S. Skolnick, A. Armitage, A. M. Afshar, and J. S. Roberts, Phys. Rev. Lett. **77**, 4792 (1996).